Performance Limitations of Power HBT Devices

Jesús Grajal de la Fuente*, Viktor Krozer**, Alfonso Campo*, Martin Schüßler+

* ETSIT, Universidad Politecnica Madrid, Ciudad Universitaria s/n, 28040 Madrid, Spain, email:jesus@gmr.ssr.upm.es

** Professur für Hochfrequenztechnik, TU Chemnitz, Reichenhainerstr. 70, D-09126 Chemnitz, Germany, email: viktor.krozer@infotech.tu-chemnitz.de

\+ Institut für Hochfrequenztechnik, TU Darmstasdt, Merckstr. 25, D-64283 Darmstadt, Germany, email: HFMWE008@hrz2.hrz.tu-darmstadt.de

Abstract— **Selfheating and thermal coupling effects are the origin of the performance limitation of amplifiers with power HBTs. It is shown that an uneven temperature distribution in individual emitter fingers and between the fingers is responsible for the limitation. A design method is proposed, which improves the temperature drain and the device reliability.**

I. Introduction

The maximum output power and power-added efficiency are important performance paramaters in applications such as mobile & satellite communications and phased-array systems. HBT devices are considered to be especially useful for microwave power amplification. The output power of HBT devices is limited by self-heating and thermal coupling effects, which degrades the high power performance of amplifier circuits and has an adverse effect on device reliabillity [1] - [6]. It is shown in the paper that an uneven temperature distribution in individual emitter fingers, as well as between the fingers is responsible for the limitation and leads to current breakdown in HBT power devices.

Therefore, the paper focuses on the thermal modelling and design aspects for the HBT device. Most device models, which include self heating effects, utilize an equivalent electrical circuit for the evaluation of the thermal operating conditions [7] [1]. Generally, the temperature is associated with the voltage in the thermal subcircuit and the power flow is associated with the current in the subcircuit, altough other implementations also exist [8]. These implementations suffer from the fact that the calculation of the temperature is not self-consistent and the temperature dependent physical parameters of the device material can not be updated during the simulation run. Another disadvantage of this approach is that an uneven distribution of the temperature across and along an emitter finger can only be approached via a discretisation of the device itself. This approach will be presented below and indeed has led to a reconsideration of the thermal model to be employed in circuit simulations. This approach is not suitable for circuit design due to the large complexity of the subcircuits.

A design method to improve the drain of the elevated temperature within the device is proposed. The design procedure is based on a physical HBT model with self-consistent device temperature calculation coupled to a circuit simulator. The results have been verified with a 2-D thermo-electrical numerical simulation tool. It can be demonstrated that an efficient temperature sinking can be achieved through the top of the device and design examples are illustrated.

II. Device Modelling

A DC and RF physical analytical HBT model has been developed [5], [13], [14], which takes into account the self-heating effects by self-consistent calculation of the Joule heating within the device. It has been implemented into a commercial circuit simulation tool. The model also includes thermal coupling between different emitter fingers and between groups of emitter fingers. Results for the power operation of HBT devices have been presented in [5]. Here we focus on the thermal characterisation.

The implemented HBT model includes the possibility of simulating the transistor's selfheating.

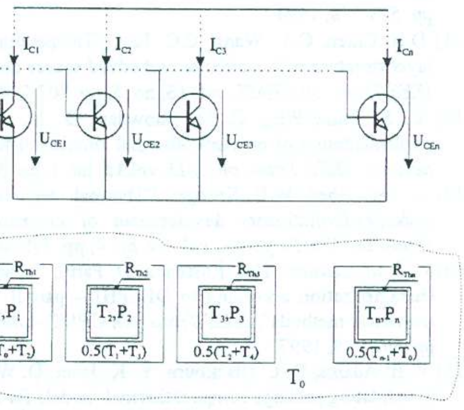

$$P_i \bullet R_{Thi} = \Delta T_i = T_i - 0.5(T_{i-1}+T_{i+1})$$

Fig. 1. Temperature calculation of thermally coupled transistors under selfheating conditions.

As shown in figure 1 the transistor is thermally coupled to its environment by a user defined thermal resistance. A number of operating modes for the calculation of the temperature effects have been implemented including thermal coupling of individual emitter fingers, thermal coupling of groups of emitter fingers, thermal coupling of individual emitter fingers without including selfheating effects of the respective fingers, and thermal coupling of groups emitter fingers without including selfheating effects of the respective individual fingers. The implemented features allow to compare the characteristic of multi-finger transistor devices with and without thermal coupling.

All temperature dependent HBT parameters including the material properties are recalculated during each iteration step. The new temperature value is calculated before the evaluation of the current and charge components.

Comparison of the experimental and simulated results for an InGaP/GaAs/InGaP DHBT are provided in fig.2 at room temperature and $300^0\,C$ ambient operating temperatures [11]. A good agreement has been achieved between experimental and simulated results. At higher operating temperatures thermal generation of carriers becomes important as indicated in fig.2.

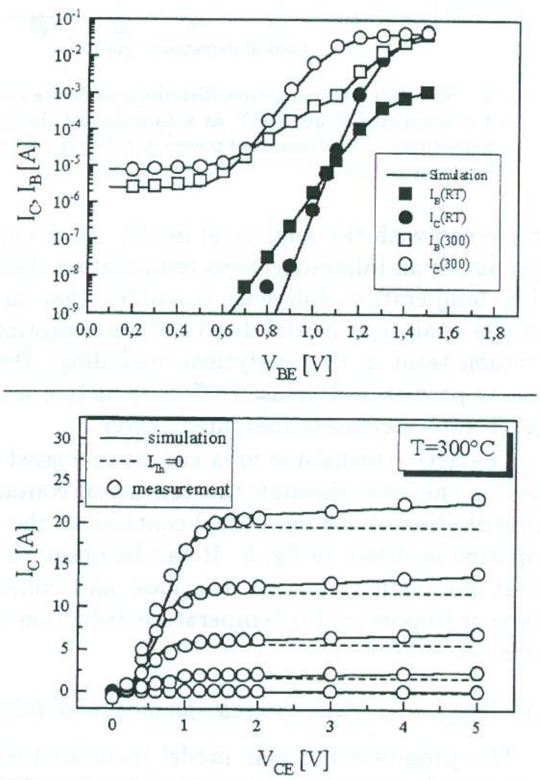

Fig. 2. Output I/V characteristic and Gummel plot for a InGaP/GaAs/InGaP DHBT. Emitter area is $4 \times 20\ \mu m^2$.

Simulations with a 2-D electro-thermal numerical model have been performed in order to verify the results of the physical analytical approach [15]. The simulation tool has been developed with special emphasis on the analysis of power HBT devices. This simulator is based on the drift-diffusion approximation, and the thermionic and thermionic-field interface conditions at the abrupt junctions [16], [17]. The model also includes the equation for the heat flow [18] in order to account for self-heating and thermal coupling between different emitter fingers. Temperature dependent material parameter tables for GaAs, AlGaAs, and InGaP compiled by [19] have been employed for the simulations. The electro-thermal calculations are performed under the assumption that all the subsystems have the same temperature [18] $T_n = T_p = T_L \equiv T$. The equations for the electron and hole current densities have to be augmented by the contribution of the temperature gradient to the current density

$$\begin{aligned} J_n &= \mu_n n \nabla E_c + qD_n \nabla n - qnD_n \nabla \ln\left(g_c m_c^{3/2}\right) + \\ &+ qnD_n^T \nabla T \\ J_p &= \mu_p p \nabla E_v - qD_p \nabla p + qpD_p \nabla \ln\left(g_v m_v^{3/2}\right) \\ &- qpD_p^T \nabla T \qquad (1) \end{aligned}$$

$$D_{n,p}^T = \frac{Q_{n,p} - \frac{3}{2}\mu_{n,p} V_T \lambda_{n,p}}{T}$$

$$Q_{n,p} = \mu_{n,p} V_T \left(r + \frac{5}{2}\right) \frac{F_{r+3/2}\left(\pm\frac{E_{f(n,p)} \mp E_{c,v}}{K_B T}\right)}{F_{r+1/2}\left(\pm\frac{E_{f(n,p)} \mp E_{c,v}}{K_B T}\right)}$$

$$\lambda_{n,p} = \frac{F_{1/2}\left(\pm\frac{E_{f(n,p)} \mp E_{c,v}}{K_B T}\right)}{F_{-1/2}\left(\pm\frac{E_{f(n,p)} \mp E_{c,v}}{K_B T}\right)}$$

where V_T is the thermal voltage, $F(*)$ is the Fermi function, μ is the carrier mobility, E_f is the quasi-Fermi level, $E_{c,v}$ stands for the conduction and valence band energy levels, respectively. At the boundaries of the device, the following boundary conditions are employed $-\kappa_{sc}(T)\nabla T \cdot \hat{n} = (T - T_0)/R_{th}$, where $\hat{n}$ is the normal vector on the surface.

III. Characterisation of temperature effects in emitter fingers

The physical analytical HBT model described above together with a thermal model for the heat dissipation through the air-bridges of multi-finger HBT structures has been used to determine the temperature distribution across and along an individual emitter finger. The intrinsic temperature has been determined by measuring the base current of the device. The thermal runaway can be explained by a local shift of the turn-on voltage of the base-emitter junction with increasing local temperature.

Thermo-electrical simulations have been performed by dividing the HBT structure into 40 HBTs with $1 \times 1\,\mu m^2$ area and connected in parallel. The simulations consider a two emitter finger device with an air-bridge. The temperature profile and the normalised current distribution are provided in fig. 3 for a power dissipation of 80 mW. In these simulations the thermal

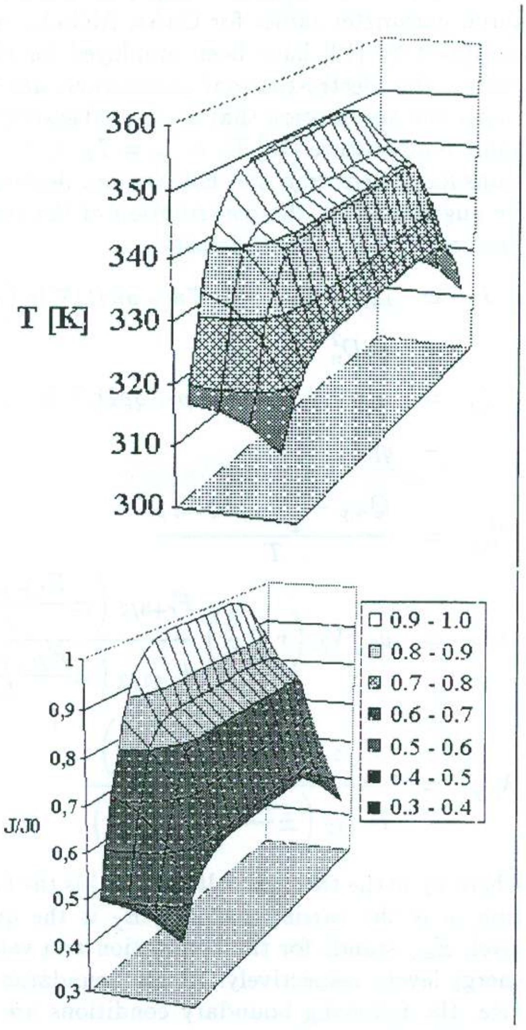

Fig. 3. Simulated temperature and current distribution in an emitter finger of a two emitter finger HBT as a function of the geometrical dimensions. The current is normalised to the maximum current. The dissipated power is $80\,mW$.

conduction through the air-bridge has been assumed comparable to the thermal convection on the sides of the emitter mesa. A temperature difference of $30^0\,C$ can be observed in fig. 3 and is the origin of the inhomogeneity in the current distribution. The dominating contribution to the total emitter current is located near the emitter side facing the second emitter finger. The thermal resistance to air of $R_{th;\mathsf{Air,bulk}} = 25 \cdot 10^3\,W/K$, originating from thermal convection, is responsible for the large temperature difference within one emitter finger. A larger value for this resistance would decrease the temperature difference but increase the overall temperature in the finger.

These results have been verified with the 2-D numerical simulation program. The metal contacts and the air-bridge are modelled as thermal resistances [20]. The sidewalls of the emitter mesa are assumed to have infinite resistance towards air. The results of simulation of a 3 emitter finger device are indicated in fig. 4 for a power dissipation of $150\,mW$ and an emitter finger area of $4 \times 20\,\mu m^2$. The results confirm the simulations

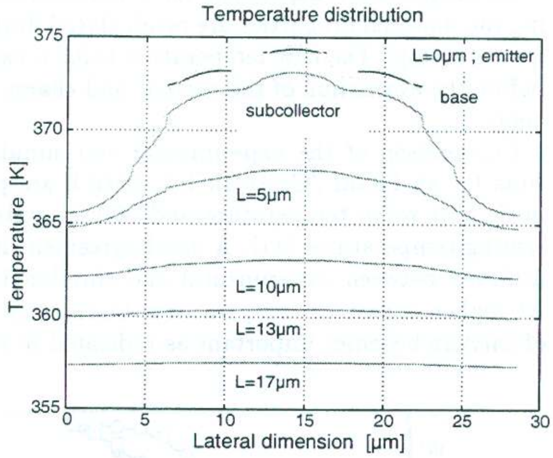

Fig. 4. Simulated temperature distribution in the cross-section of a 3 emitter finger HBT as a function of the geometrical dimensions. The dissipated power is $150\,mW$. The substrate thickness is $100\,\mu m$.

perfomed with the analytical model. Each emitter finger shows an inhomogeneous temperature distribution. The temperature difference is smaller than in the case of the analytical model due to the assumption of convection term in the analytical modelling. Both simulators predict a decreased effective active area of the HBT with increased dissipated power.

The active transistor area can be increased by dissipating the heat through the top metal contacts. The contribution of the individual contacts to the heat dissipation is shown in fig. 5. It can be observed that the heat conduction through the base and collector contacts is important for temperature reduction within th edevice.

A. Design approach to multi-finger power HBT devices

The proposed thermal model includes the thermal coupling between several emitter fingers, the thermal drain through the contacts, and the thermal distribution within the active device area. An uneven distribution is modelled by moving the thermal source away from the center of the cross-section of the device. The thermally induced current breakdown within one emitter finger is modelled by modifying the effective active area of the emitter. An equivalent circuit of the thermal circuit is presented in fig.6. The sources left and right to the device represent the temperature coupling from neighbouring fingers.

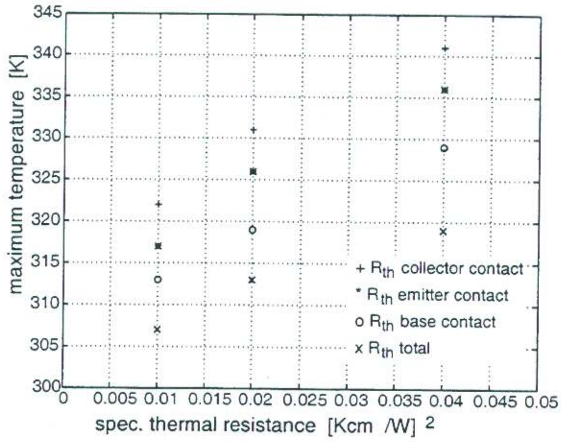

Fig. 5. Simulated temperature increase as a function of thermal resistance for the individual contacts. The dissipated power is $150\,mW$. The substrate thickness is $100\,\mu m$.

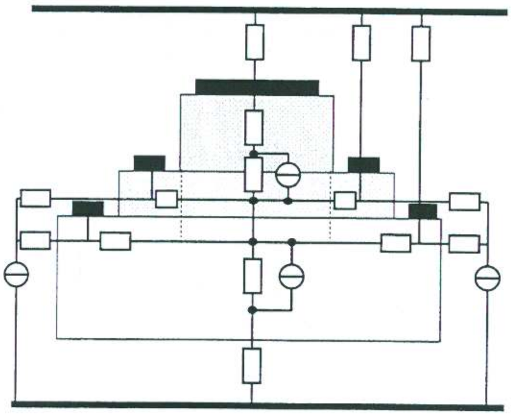

Fig. 6. Thermal equivalent circuit for the HBT device.

The effective thermal resistance of a HBT device can be obtained from calculations of the capacitance of an equivalent electrical structure. The geometrical structure of multi-finger HBT devices resembles that of multiple coupled striplines with inhomogeneous layered dielectric [12]. The equivalence between the electrical and thermal quantities can be utilised for the determination of the coupling coefficient between adjacent emitter fingers. Utilizing the equivalence between the dielectric constant and the thermal conductivity and between the electrical capacitance and the thermal conductance, the formulas derived for the coupling capacitance in [12] can be used to obtain an equivalent relation for the coupling thermal conductance of two emitter fingers with equal width.

The design goal is to maximize the active device area with a uniform temperature distribution and small temperature increase. The design procedure starts with the definition of the emitter area as a function of maximum junction temperature and effective thermal resistance of one emitter finger for a given dissipated power. The base and collector contact areas are determined such that the maximum junction temperature of an individual emitter finger does not increase for a prescribed elevated ambient temperature . The number of fingers are chosen according to the total output power. Finally, the spacing between the emitter fingers is evaluated such that the effective thermal resistance of the overall structure is minimized. This requires the calculation of the thermal coupling coefficient.

B. Conclusions

Results for the temperature distribution across and along emitter fingers of multi-finger HBT devices are discussed. The simulations have been performed with a physical HBT model self-consistently including thermal effects. These simulations have been verified with 2-D electro-thermal numerical simulations. It could be shown that heat dissipation through the air-bridge and the other contacts is essential for low operating temperatures as well as homogeneous distribution of temperature in the emitter finger. Thermal runaway can be explained by the nonhomogeneous temperature and current distribution.

References

[1] C.-W. Kim, N. Goto, and K. Honjo, "Thermal behavior depending on emitter finger and substrate configurations in power heterojunction bipolar transistors," *IEEE Trans. Electronic Devices*, vol. ED-45, no. 6, pp. 1190–5, 1998.

[2] W. Liu, S.-K. Fan, T. Henderson, and D. Davito, "Temperature dependence of current gains in *gainp/gaas* and *algaas/gaas* heterojunction bipolar transistors," *IEEE Trans. Electronic Devices*, vol. ED-40, pp. 1351–3, 1993.

[3] A. Marty, T. Campy, J. Tasselli, D.L. Pulfrey, and J.P. Bailbe, "A self-consistent dc-ac two-dimensional electrothermal model for *gaalas/gaas* microwave power hbt's," *IEEE Trans. Electronic Devices*, vol. ED-40, pp. 1202–1210, 1993.

[4] M.E. Hafizi, W. E. Stachina, R. A. Metzger, P. A. Mcdonald, and F. Williams Jr., "Temperature dependence of dc and rf characterisitcs of *alinas/gainas* hbt's," *IEEE Trans. Electronic Devices*, vol. ED-40, no. 9, pp. 1583–7, 1993.

[5] V. Krozer, M. Ruppert, M. Schüßler, K. Fricke, W.-Y. Lee, and H. L. Hartnagel, "Calculation of the power capabilities of hbt amplifiers based on a new physical hbt model," *J. Microwave and Millimeter-Wave Computer-Aided Eng.*, vol. 6, no. 4, pp. 270–280, 1996.

[6] J. Dupuis, R. Hajji, F. M. Ghannouchi, K. Saab, and S. Lavallée, "A new dc model of hbt's including self-heating effects suitable for circuit simulation," *IEEE Trans. Electronic Devices*, vol. ED-42, no. 12, pp. 2036–2042, 1995.

[7] J.J. Liou, T. J. Jenkins, L.L. Liou, R. Neidhard, D. W. Barlage, R. Fitch, J. P. Barrette, M. Mack, C. A. Bozada, R. H. Y. Lee, R. W. Dettmer, and J. S. Sewell, "Bias, frequency, and area dependencies of high frequency noise in AlGaAs/GaAs HBT's," *IEEE Trans. Electronic Devices*, vol. ED-43, no. 1, pp. 116–121, 1996.

[8] C. H. Diaz, S.-M. Kang, and C. Duvvury, "Circuit-level electrothermal simulation of electrical overstress failures in advanced mos i/o protection devices," *IEEE Trans. Computer-Aided Design*, vol. CAS-13, no. 4, pp. 482–493, 1994.

[9] V. Rizzoli, A. Lipparini, A. Costanzo, and V. Frontini, "Three-dimensional computation of the thermal parameters of multiple-gate power fets," in *Proc. 23rd European Microwave Conf.*, Madrid, Spain, 1993, pp. 698–700.

[10] W. Liu and A. Khatibzadeh, "The collapse of current gain in multi-finger heterojunction bipolar transistors: Its substrate temperature dependence, instability criteria, and modeling," *IEEE Trans. Electronic Devices*, vol. ED-41, no. 10, pp. 1698–1707, 1994.

[11] M. Schüßler, "Neue Konzepte der Technologie, Zuverlässigkeit und Anwendung von GaAs HBT," *Ph.D. thesis*, TU Darmstadt, Darmstadt, Germany, 1997.

[12] B.M. Das and K.V.S.V.R. Prasad, "A Generalized Formulation of Electromagnetically Coupled Striplines," *IEEE Trans. Microwave Theory & Techn.*, vol. MTT-32, no. 11, 1984.

[13] V. Krozer, M. Schüßler, J. Grajal, and H. L. Hartnagel, "Thermal coupling in multifinger heterojunction bipolar devices," in *27th European Microwave Conference*, Jerusalem, Israel, 8-12 Sept. 1997.

[14] V. Krozer, M. Ruppert, W.Y. Lee, J. Grajal, A. Goldhorn, M. Schü ler, K. Fricke, and H. L. Hartnagel, "A physics-based temperature-dependent spice model for the simulation of high temperature microwave performance of hbt's and experimental results," in *1994 IEEE MTT-S, Intern. Microwave Symp. Dig.*, San Diego, USA, Mai 23-27,1994.

[15] J. Grajal de la Fuente, *Modelado Fisico de Dispositivos Basados en Heterostructuras para Aplicaciones de Radiofrecuencia*, Ph.D. thesis, Univ. Politecnica de Madrid, Madrid, Spain, 1998.

[16] K. Horio and H. Yanai, "Numerical modeling of heterojunctions including the thermionic emission mechanism at the heterojunction interface," *IEEE. Trans. on Electron Devices*, vol. 37, no. 4, pp. 1093–1098, Apr. 1990.

[17] K. Yang, J. R. East, and G. I. Haddad, "Numerical modeling of abrupt heterojunctions using a thermionic emission boundary condition," *Solid-State Electronics*, vol. 36, no. 3, pp. 321–330, 1993.

[18] U. lindefelt, "Heat generation in semiconductor devices," *Journal of Applied Physiscs*, vol. 15, no. 2, pp. 942–957, Jan. 1994.

[19] V. Krozer, *Simulation und Modellierung von THz-Schottky Dioden und Heterostruktur-Bipolar-Transistoren hergestellt auf Verbindungshalbleitern*, Technische Hochschule Datmstadt, Darmstadt, Germany, 1997.

[20] J.J. Liou, L.L. Liou, C.I. Huang, and B. Bayraktaroglu, "A physics-based, analytical heterojunction bipolar transistor model including thermal and high-current effects," *IEEE Trans. Electronic Devices*, vol. ED-40, pp. 1570–7, 1993.